0026-895X/02/6204-795–805$7.00
MOLECULAR PHARMACOLOGY
Copyright © 2002 The American Society for Pharmacology and Experimental Therapeutics
Mol Pharmacol 62:795–805, 2002

Vol. 62, No. 4
1278/1011898
Printed in U.S.A.

Kinetics and Crystal Structure of Catechol-*O*-Methyltransferase Complex with Co-Substrate and a Novel Inhibitor with Potential Therapeutic Application

MARIA JOÃO BONIFÁCIO, MARGARIDA ARCHER, MARIA L. RODRIGUES, PEDRO M. MATIAS, DAVID A. LEARMONTH, MARIA ARMÉNIA CARRONDO, and PATRÍCIO SOARES-DA-SILVA

Department of Research and Development, BIAL, S. Mamede do Coronado, Portugal (M.J.B., D.A.L., P.S.S.); Instituto de Tecnologia Química e Biológica-Universidade Nova de Lisboa, Oeiras, Portugal (M.A., M.L.R., P.M.M., M.A.C.); and Instituto de Biologia Experimental e Tecnológica, Oeiras, Portugal (M.A., M.L.R.)

Received February 27, 2002; accepted June 27, 2002

This article is available online at http://molpharm.aspetjournals.org

ABSTRACT

Catechol-*O*-methyltransferase (COMT; E.C. 2.1.1.6) is a ubiquitous enzyme in nature that plays an important role in the metabolism of catechol neurotransmitters and xenobiotics. In particular, inactivation of drugs such as L-3,4-dihydroxyphenylalanine (L-DOPA) via *O*-methylation is of relevant pharmacological importance, because L-DOPA is currently the most effective drug used in the treatment of Parkinson's disease. This justified the interest in developing COMT inhibitors as potential adjuncts to L-DOPA therapy. The kinetics of inhibition by BIA 3-335 (1-[3,4-dihydroxy-5-nitrophenyl]-3-(*N*-3′-trifluormethylphenyl)-piperazine-1-propanone dihydrochloride) were characterized using recombinant rat soluble COMT. BIA 3-335 was found to act as a potent, reversible, tight-binding inhibitor of COMT with a K_i of 6.0 ± 1.6 nM and displaying a competitive inhibition toward the substrate binding site and uncompetitive inhibition toward the *S*-adenosyl-L-methionine (SAM) binding site. The 2.0-Å resolution crystal structure of COMT in complex with its cosubstrate SAM and a novel inhibitor BIA 3-335 shows the atomic interactions between the important residues at the active site and the inhibitor. This is the first report of a three-dimensional structure determination of COMT complexed with a potent, reversible, and tight-binding inhibitor that is expected to have therapeutic applications.

Catechol-*O*-methyltransferase (COMT; EC 2.1.1.6) catalyzes the methylation of small molecules containing a catechol structure, being responsible for the elimination of catechol-based neurotransmitters, catechol steroids, and xenobiotic catechols (Lautala et al., 2001). In humans and laboratory animals, COMT is present in all tissues studied (Lundström et al., 1995); highest activities are found in liver, kidney, and gastrointestinal tract (Männistö et al., 1992; Männistö and Kaakkola, 1999). It is present as membrane-bound and soluble (S-COMT) forms, both encoded by a single gene using different promoters and translational regulation (Tenhunen and Ulmanen, 1993; Tenhunen et al., 1993, 1994). Both forms are present in practically all tissues in which S-COMT is the predominant form (Rivett et al., 1983; Karhunen et al., 1994; Ding et al., 1996), except in human brain, where membrane-bound COMT dominates (Tenhunen et al., 1993, 1994). Both the rat and human S-COMT have 221 amino acids with molecular masses of 24.7 and 24.4 kDa, respectively, and share 81% amino acid sequence identity (Salminen et al., 1990; Lundström et al., 1991). The resolution of the atomic structure and sequence comparisons revealed that all residues important for the binding of substrates and for the catalytic site are conserved in human and rat S-COMT (Vidgren et al., 1994; Lotta et al., 1995).

The main clinical interest in COMT results from the possibility of using COMT inhibitors as adjuncts in the therapy of Parkinson's disease with L-3,4-dihydroxyphenylalanine (L-DOPA) (Männistö and Kaakkola, 1989, 1990). This disease is characterized by progressive degeneration of the dopaminergic nigrostriatal pathways; at present, the most effective therapy is dopamine replacement with L-DOPA plus a peripheral aromatic L-amino acid decarboxylase inhibitor. Under these circumstances, the methylation of L-DOPA becomes the major metabolization route in the periphery and only 5 to 10% of administered L-DOPA reaches the brain (Männistö and Kaakkola, 1990). The inhibition of COMT would increase

This work was supported in part by grant P003-P31B-02/97 BIAL-COMT from Agência de Inovação and fellowships PRAXIS XXI/BIC/17185/98 (M.L.R) and PRAXIS XXI/BPD/17265/98 (M.A.).

M.J.B. and M.A. contributed equally to the study.

ABBREVIATIONS: COMT, catechol-*O*-methyltransferase; S-COMT, soluble catechol-*O*-methyltransferase; L-DOPA, L-3,4-dihydroxyphenylalanine; BIA 3-335, 1-[3,4-dihydroxy-5-nitrophenyl]-3-[*N*-3′-trifluoromethyl-phenyl]-piperazine-1-propanone; SAM, *S*-adenosyl-L-methionine; MT, methyltransferases.

the bioavailability of L-DOPA, prolong its half-life, and decrease the formation of 3-*O*-methyl-L-DOPA. These effects are indeed observed when tolcapone (Zürcher et al., 1990) and entacapone (Männistö et al., 1988), two tight-binding COMT inhibitors, were administered to human volunteers (Bonifati and Meco, 1999). Both inhibitors were also shown to enhance and extend the therapeutic effect of L-DOPA in patients with advanced and fluctuating Parkinson's disease (Rajput et al., 1997; Waters et al., 1997; Rinne et al., 1998). Furthermore, COMT inhibition led to some cognition-improving effects (Gasparini et al., 1997) and, in animal models of depression, some beneficial effects were also observed (Männistö et al., 1995; Moreau et al., 1994). The three-dimensional structure of the COMT in complex with these inhibitors has never been reported. The only structure available is the one of COMT complexed with SAM and 3,5-dinitrocatechol (Vidgren et al., 1994), which, however, has no therapeutic application (Bonifati and Meco, 1999).

BIA 3-335 (Fig. 1) is a novel, highly selective, and potent COMT inhibitor that has been synthesized to preferentially act as a peripheral inhibitor (Learmonth and Soares-da-Silva, 2002). Here, we report on the kinetics of inhibition of a rat recombinant form of soluble COMT by BIA 3-335 and on the crystal structure, at 2.0-Å resolution, of the enzyme complexed with SAM and BIA 3-335. The three-dimensional structure reveals the interactions at the catalytic site between the enzyme and a large inhibitor.

Materials and Methods

Animals. Naval Medical Research Institute mice (Harlan-Interfauna Ibérica, Barcelona, Spain), 60 days old and weighing 25 to 30 g, were used in all experiments. Mice were kept under controlled environmental conditions (12-h light/dark cycle and room temperature 22 ± 1°C) with food and tap water allowed ad libitum. All animals interventions were performed in accordance with the European Directive number 86/609, and the rules of the National Institutes of Health *Guide for the Care and Use of Laboratory Animals* (http://oacu.od.nih.gov/regs/guide/guidex.htm).

In Vivo Studies. BIA 3-335 and entacapone were given by gastric tube (30 mg/kg in saline with 10% Tween 80) to mice fasted overnight. Thereafter, at defined intervals (1 and 6 h), animals were anesthetized with sodium pentobarbital (60 mg/kg) and perfused through the left ventricle with 0.9% (w/v) NaCl. Livers and brains were immediately removed and homogenized in 5 mM sodium phosphate buffer, pH 7.8, at 4°C with a Teflon homogenizer (Heidolph, Schwabach, Germany). The homogenates were used for the COMT assay as described below.

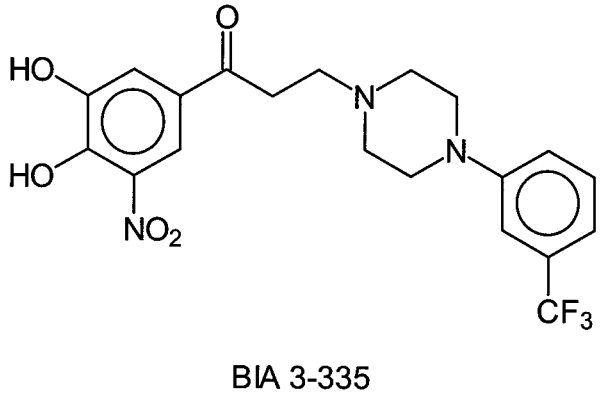

Fig. 1. Chemical structure of COMT inhibitor BIA 3-335 (1-[3,4-dihydroxy-5-nitrophenyl]-3-[*N*-3′-trifluoromethyl-phenyl]piperazine-1-propanone).

Enzyme Preparation. Recombinant rat soluble-COMT was produced in *Escherichia coli* and was purified to homogeneity as described previously (Bonifácio et al., 2001; Rodrigues et al., 2001). The recombinant S-COMT was quantified with the BioRad standard protein assay (BioRad, Hercules, CA) using a standard curve of bovine serum albumin (50–250 μg/ml).

Enzyme Assay. The general procedure for measuring COMT activity was based on the determination of the metanephrine formed by the *O*-methylation of epinephrine, as described previously (Borges et al., 1997; Bonifácio et al., 2000). Enzyme activity was determined in 100 μM $MgCl_2$, 1 mM EGTA, and 10 mM sodium phosphate buffer, pH 7.2. The concentrations of the enzyme, epinephrine, SAM, and inhibitors varied according to the respective experiment performed. Metanephrine was measured by HPLC with electrochemical detection, as described previously (Borges et al., 1997; Bonifácio et al., 2000).

Kinetic Measurements and Reversibility Studies. In experiments designed to evaluate the kinetic parameters K_i and K_{cat}, S-COMT (260–1168 nM) was incubated with epinephrine (1000 μM), SAM (500 μM), and BIA 3-335 (0–750 nM). In these experiments, reactions were initiated by the addition of substrate. The steady state between the enzyme and the inhibitor was evaluated by using 520 nM S-COMT in the absence or in the presence of 300 nM of BIA 3-335 and by starting the reaction with the addition of the enzyme or the substrate (1000 μM epinephrine). In the experiments designed to evaluate the inhibitory mechanism, 520 nM S-COMT were incubated with 60 to 3000 nM of BIA 3-335 in the presence of either different epinephrine (100, 500, and 1000 μM) or SAM (10, 40, and 100 μM) concentrations. In the latter experiments, reactions were started by the addition of the enzyme. The reversibility studies were performed as follows: samples contained 520 nM S-COMT with or without 1000 nM BIA 3-335; after a 20-min preincubation at 37°C, samples were applied onto a PD-10 column (Amersham Biosciences, Little Chalfont, Buckinghamshire, UK) after withdrawing 500 μl for assessing total inhibition. Eluate containing protein was collected and enzyme activity was determined in the samples collected before and after gel filtration using 2000 μM epinephrine. The activity of the vehicle before gel filtration was 270 ± 8/h and after gel filtration was 229 ± 6/h.

Data Analysis. K_i values were determined by fitting the steady-state rate values obtained for various enzyme and inhibitor concentrations to the equation (Cha, 1975; Williams and Morrison, 1979)

$$v = \frac{K_{cat}S}{2(K_m + S)}\left[(\varepsilon E - K_i^* - I) + \sqrt{(K_i^* + I + \varepsilon E)^2 - 4I\varepsilon E}\right]$$

In this equation, E is the total enzyme concentration in arbitrary units; ϵ represents the fraction of E that is active, thus the molar equivalency; I is the total inhibitor concentration; K_{cat} is the catalytic number, which gives the number of molecules of substrate transformed into product per catalytic center per unit of time; and K_i^* is an apparent enzyme-inhibitor dissociation constant value. The true K_i can be determined by dividing the K_i^* by $(1 + S/K_m)$. K_m and V_{max} values for COMT activity were calculated from nonlinear regression analysis using Prism version 3.02 (GraphPad Software Inc., San Diego, CA).

IC_{50} values were determined by fitting the experimental data to the respective equations using GraphPad Prism. Geometric means are given with 95% confidence intervals and arithmetic means are given with S.E.M. Statistical analysis was performed by one-way analysis of variance followed by Newman-Keuls multiple comparison test.

Crystallization and Data Collection. The purified protein was preincubated with the magnesium ion, the cosubstrate SAM, and the inhibitor BIA 3-335 before the crystallization assays were set. The crystals were obtained using polyethylene glycol 6000 as precipitant.

A diffraction data set, measured at room temperature, was collected using in-house equipment. The crystal belongs to space group $P3_221$, with unit cell dimensions of a = b = 51.49 Å and c = 168.29 Å (Rodrigues et al., 2001).

Structure Determination and Refinement. The COMT structure complexed with SAM and the inhibitor BIA 3-335 was refined with crystallography and NMR systems software (Brunger et al., 1998) using the coordinates of rat COMT (Protein Data Bank entry: 1vid) (Vidgren et al., 1994) as initial model. Before the refinement procedure, 5% of randomly chosen reflections were flagged for R-free calculations. The refinement was initially carried out using rigid-body followed by simulated annealing/slow cooling protocols. All low-resolution data were included in the crystallographic refinement and bulk solvent correction was applied. Refinement started using data up to 3 Å and was gradually extended to ~2-Å resolution. The electron density maps were calculated with compressible Navier-Stokes equations and inspected with the program TURBO (Roussel and Cambilau, 1989). The initial 2F(obs)-F(calc) and F(obs)-F(calc) calculated Fourier maps showed very well defined density for the cosubstrate SAM and for the nitrocatechol part of the inhibitor BIA 3-335. The density for the rest of the inhibitor gradually appeared after several cycles of model building and energy minimization calculations. The coordinates of the BIA 3-335 structure determined by X-ray analysis were used to fit this compound into the electron density maps. Water molecules were added in the latter stages of refinement and the individual restrained temperature factors were refined. The coordinates of the final refined model/complex COMT-SAM-BIA3-335 have been deposited in the Protein Data Bank with the Protein Data Bank accession code 1H1D.

Crystallization and X-Ray Structure Resolution of BIA 3-335 Molecule. The compound BIA 3-335 was crystallized by the vapor diffusion method using a solvent/precipitant pair of 100% methanol against 80% methanol/20% water. The small molecule structure was determined by direct methods using SHELXS-97 (Sheldrick, 1997). All nonhydrogen atoms were refined with anisotropic thermal displacement parameters. The hydrogen atoms were placed in calculated positions and refined using either the riding or the rotating group models (Sheldrick, 1997). The terminal CF_3 group was modeled using a 2-fold disorder scheme (0.63/0.37) and the anion site was found to contain a mixture of Br^- and Cl^-. Because of convergence problems in the refinement, the relative proportions of these ions were determined by trial and error (wR_2 minimization) to be 0.315 and 0.685, respectively.

Reagents. Epinephrine (bitartrate salt), DL-metanephrine, and SAM were purchased from Sigma Chemical Co (St Louis, MO). BIA 3-335 and entacapone were synthesized in the Laboratory of Chemistry (BIAL, Portugal), with purities >99.5%.

Results

In Vivo COMT Inhibition. Incubation of mouse liver and brain COMT assay mixture in the presence of increasing concentrations of epinephrine resulted in a concentration-dependent formation of metanephrine, with K_m (micromolar) and V_{max} (nanomoles per milligram of protein per hour) values of, respectively, 5.1 ± 1.9 and 24.9 ± 2.1 in liver and 1.6 ± 0.4 and 1.2 ± 0.1 in brain. Saturation curves were also performed for the methyl donor, SAM. The kinetic parameters, K_m (micromolar) and V_{max} (nanomoles per milligram of protein per hour), obtained for SAM were 15.2 ± 3.1 and 46.2 ± 1.7, respectively, in liver and 2.4 ± 0.3 and 1.2 ± 0.1, respectively, in brain. From these results, saturating concentrations of adrenaline (100 μM) and SAM (250 μM) were chosen for subsequent studies. The in vivo inhibitory potency of BIA 3-335 and entacapone was evaluated in experiments in which mice were given the COMT inhibitors (30 mg/kg) 1 and 6 h before killing. As shown in Fig. 2, the inhibitory effect of entacapone upon liver COMT is a time-dependent effect and is markedly attenuated at 6 h. By contrast, the inhibitory effect of BIA 3-335 at 1 h was identical to that observed at 6 h after the administration. Both compounds failed to affect brain COMT activity.

Kinetic Parameters of Recombinant S-COMT. The activity dependence of recombinant rat S-COMT with the en-

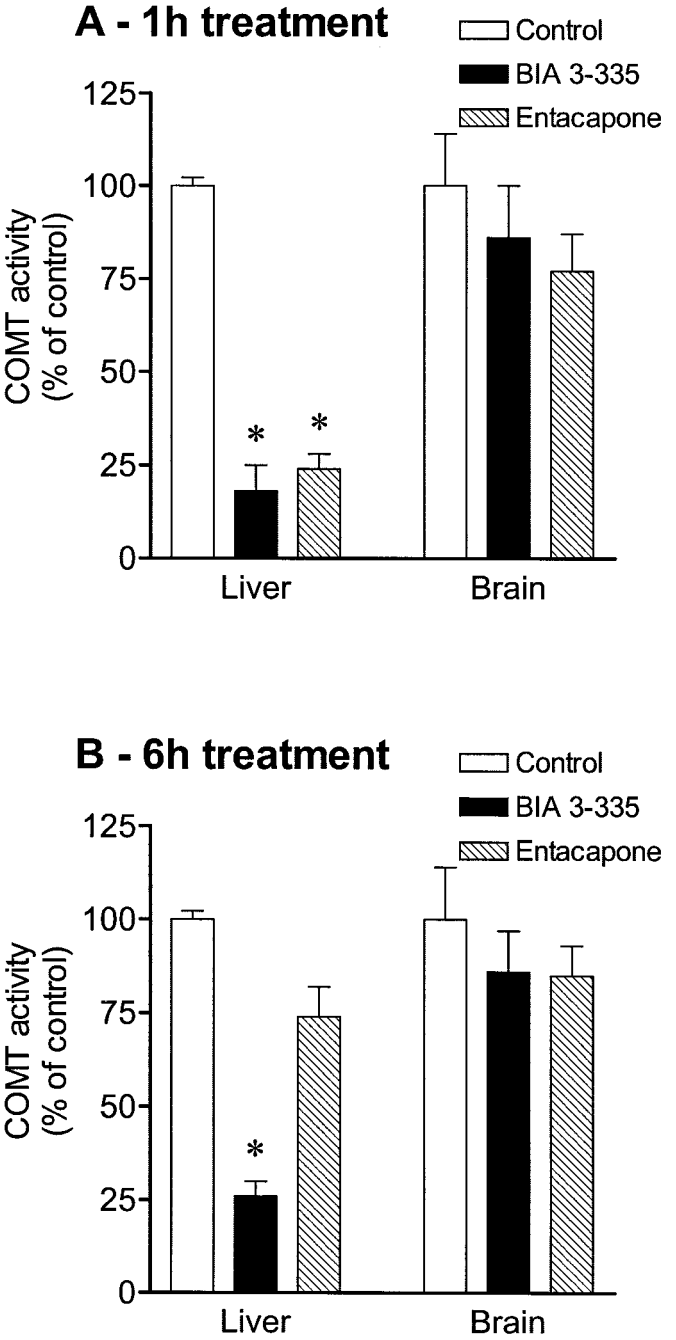

Fig. 2. COMT activity in homogenates of mouse liver and brain, determined at 1 h (A) and 6 h (B) after the oral administration of vehicle, BIA 3-335 (30 mg/kg) and entacapone (30 mg/kg). Each bar represents the mean of four independent experiments. Vertical lines represent S.E.M. Significantly different from the corresponding control values (* $P < 0.05$). The rate of formation of metanephrine (nanomoles per milligram of protein per hour) in control conditions was 4.38 ± 0.10 and 0.15 ± 0.02 in liver and brain, respectively.

zyme concentration and incubation time was determined, and a linear correlation was observed for protein concentrations up to 1.5 μM (Fig. 3A) and incubation times up to 15 min (Fig. 3B). According to these results, 5-min incubation and either 260 or 520 nM S-COMT were the conditions chosen for all the ensuing experiments. The incubation of S-COMT with different concentrations of either epinephrine or SAM resulted in the concentration-dependent formation of metanephrine as shown in Fig. 4, A and B, respectively. The kinetic parameters derived from these curves were: K_m = 578 (95% confidence limit, 471, 684) μM, V_{max} = 529 ± 16/h for epinephrine and K_m = 30 (22, 37) μM, V_{max} = 377 ± 11/h for SAM.

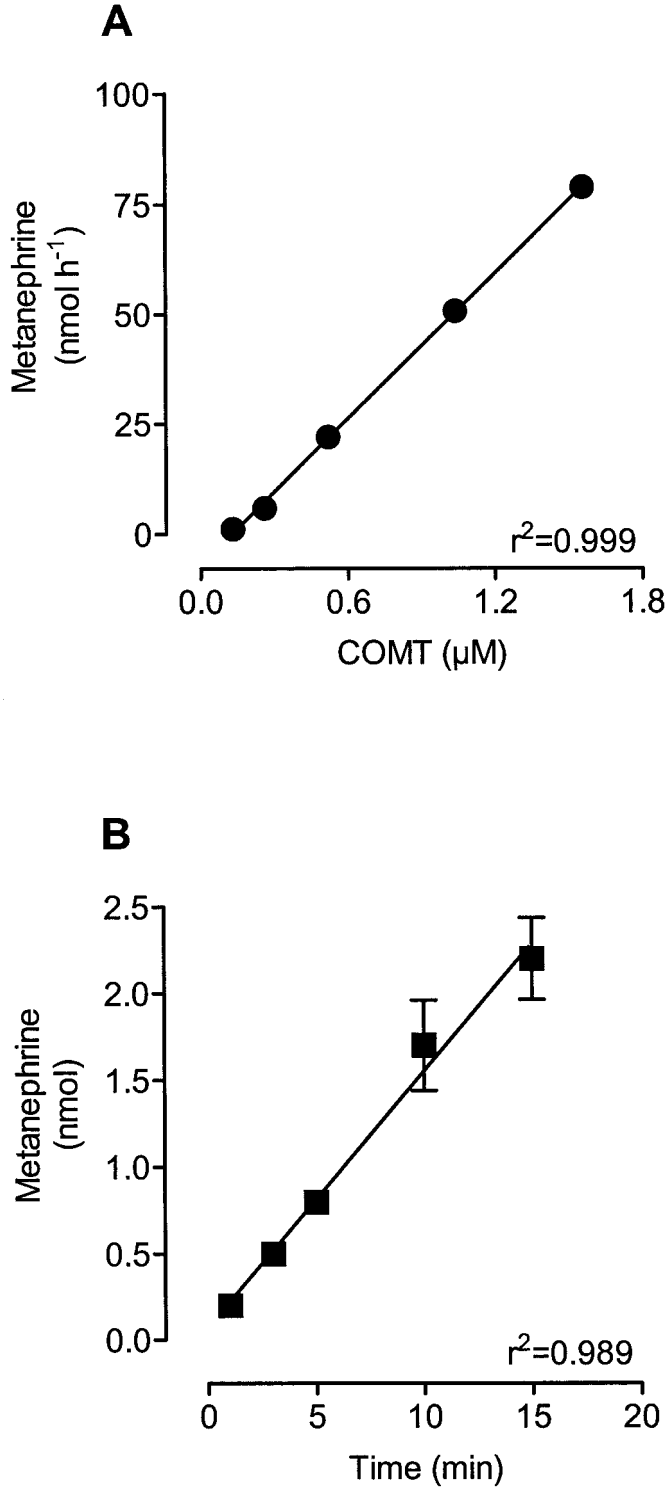

Fig. 3. *O*-Methylation of epinephrine as a function of S-COMT concentration and of incubation time. A, the enzyme (0.013–1.8 μM) was incubated for 5 min with 500 μM SAM and 1 mM epinephrine. B, S-COMT (280 nM) was incubated with 500 μM SAM and 1 mM epinephrine for 1 to 15 min. Symbols represent a single experiment performed in triplicate.

S-COMT Inhibition by BIA 3-335. In the presence of 520 nM S-COMT, increasing concentrations of BIA 3-335 produced concentration-dependent decreases in the *O*-methylation of epinephrine (Fig. 5) with an IC_{50} value of 447 nM. The fact that this compound inhibited COMT activity at concentrations comparable with that of the enzyme suggests that it may behave as a tight-binding inhibitor (Morrison, 1969). Thus all subsequent kinetic analyses were carried out according to the tight-binding theory (Williams and Morrison, 1979). The reversibility of the BIA 3-335 interaction with S-COMT was evaluated by gel filtration. As can be observed in Fig. 6, before gel filtration BIA 3-335 inhibited 67% of S-COMT activity. However, the inhibition was completely reversed after gel filtration. To determine the rate at which equilibrium is obtained between the enzyme and the enzyme-inhibitor complex, the formation of metanephrine was measured as a function of time under three different experimental conditions: 1) by starting the reaction with the addition of the substrate to the enzyme in the absence of BIA 3-335; 2) by starting the reaction with the addition of the substrate after a 20-min preincubation of BIA 3-335 with COMT, and 3) by starting the reaction with the addition of the enzyme to the reaction mixture containing the substrate plus BIA 3-335. In the absence of BIA 3-335, product formation increased linearly with time at a rate of 0.296 ± 0.010 nmol/min (Fig. 7). In the presence of BIA 3-335, product formation also increased linearly with time. However, rates of metanephrine formation obtained with (0.217 ± 0.009 nmol/min) and without preincubation (0.217 ± 0.014 nmol/min) were lower ($P < 0.05$) than in the absence of BIA 3-335. Similarity of rates of metanephrine formation obtained with or without preincubation (Fig. 7), suggest that equilibrium involving inhibitor and substrate was established very rapidly.

Mechanism of Enzyme Inhibition. To determine the type of inhibition produced by BIA 3-335, IC_{50} values were determined at increasing concentrations of epinephrine and SAM. An increase in epinephrine concentration resulted in a linear increase in IC_{50} values (Fig. 8A), indicating a competitive type of inhibition toward the substrate. On the other hand, when the concentration SAM was varied, a linear increase in IC_{50} values was observed with the inverse of SAM concentration (Fig. 8B), indicating an uncompetitive inhibition toward the SAM binding site. Steady-state rate values were also obtained for various enzyme and inhibitor concentrations at a fixed substrate concentration. The plot of v against E at various levels of I (Ackermann-Potter plot) was characterized by asymptotic concave-up curves (Fig. 9), which are diagnostic of tight binding inhibition. This further confirms BIA 3-335 tight-binding nature. The parameters K_i^*, K_{cat}, and ϵ were estimated by nonlinear regression and are represented in Table 1 together with the true K_i value derived from K_i^*.

Structure Analysis. The final model of COMT complexed with SAM and BIA3-335 was refined to 2-Å resolution using diffraction data from a crystal measured at room tempera-

ture. Details of the data collection and refinement statistics are summarized in Table 2. The model of the ternary complex comprises 214 residues, 85 water molecules, the cosubstrate SAM, the inhibitor BIA 3-335, and a Mg^{2+} ion and was refined to *R*-factor of 17.4% and free R-factor of 19.8%. To have a better accuracy for the BIA 3-335 molecule, its structure was independently determined by X-ray diffraction data analysis. Relevant parameters of crystal data and structure refinement statistics are presented in Table 3. The first two N-terminal and the last five C-terminal amino acid residues are not visible in the electron density maps and hence were

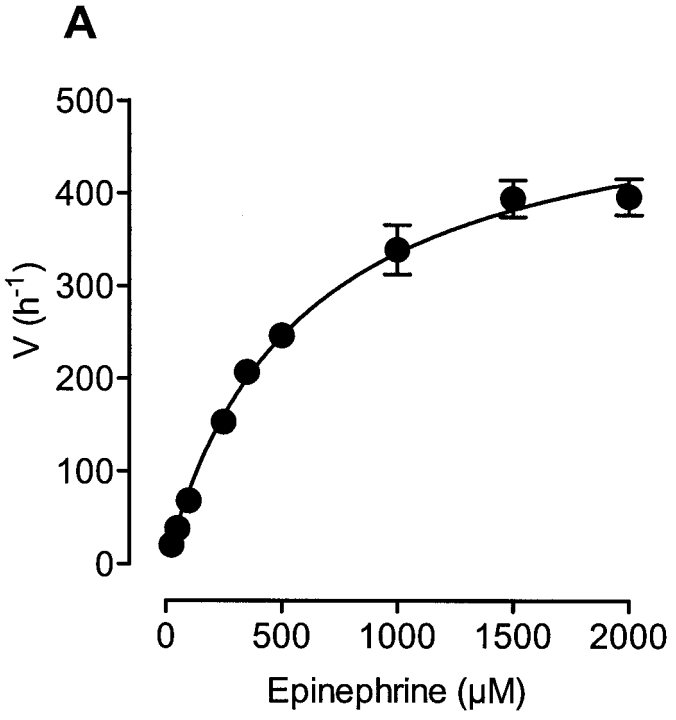

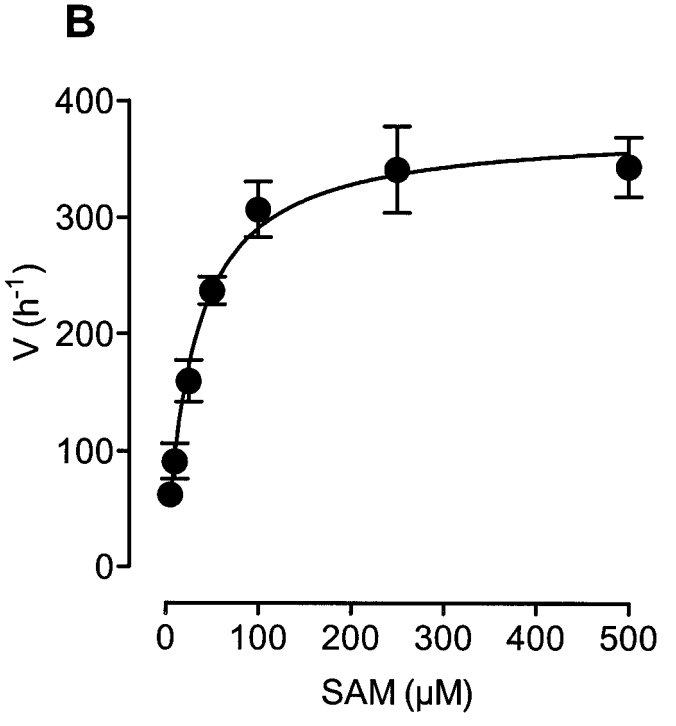

Fig. 4. *O*-Methylation of epinephrine by S-COMT. S-COMT (260 nM) was incubated with different concentrations of epinephrine in the presence of 500 μM SAM (A) or different concentrations of SAM in the presence of 1000 μM epinephrine (B). Symbols represent the average of two to three independent determinations. Vertical lines represent S.E.M.

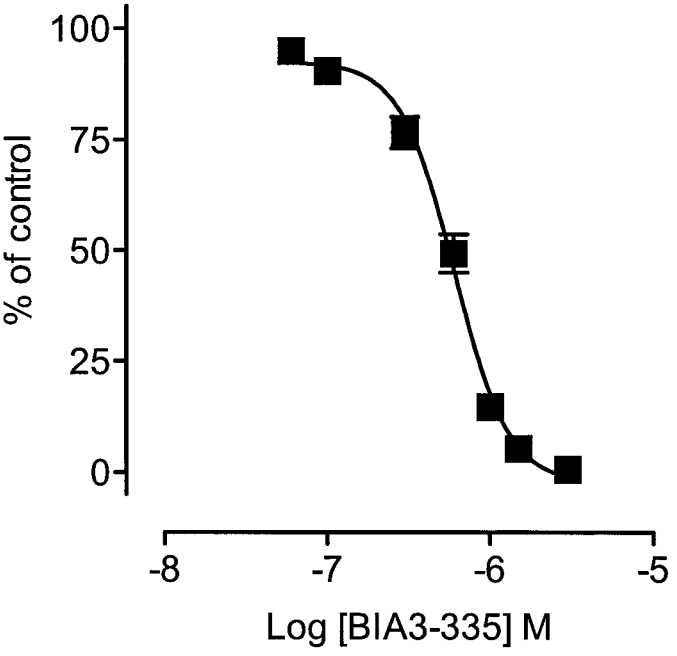

Fig. 5. S-COMT inhibition by BIA 3-335. S-COMT was incubated with increasing concentrations of BIA 3-335 in the presence of 1000 μM epinephrine. Symbols represent the average of six independent determinations. Vertical lines represent S.E.M.

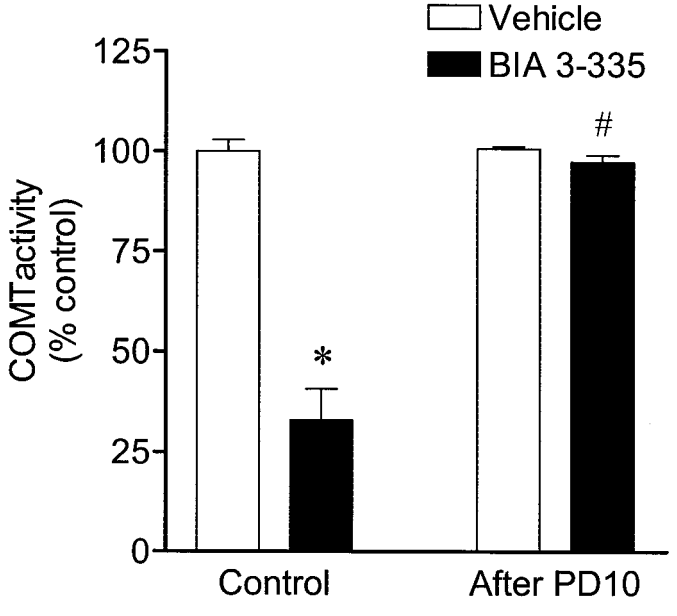

Fig. 6. Reversibility of S-COMT inhibition by BIA 3-335. S-COMT activity in the absence (control) and in the presence of 1000 nM BIA 3-335 (BIA 3-335) before and after being passed on PD-10 columns. Each bar represents the mean of two independent experiments each performed in duplicate. Vertical lines represent S.E.M. Significantly different from the corresponding control values (*$P < 0.05$) and values for BIA 3-335 before being passed on PD-10 columns (#$P < 0.05$).

not included in the model. The density for SAM is very well defined in the first calculated map, reflected by its low atomic temperature factors (B_{avg} of 17.2 Å^2). The active site occupied by the inhibitor BIA 3-335 has clear density for nitrocatechol (dihydroxynitrophenyl) (B_{avg} of 27.1 Å^2) and propanone (B_{avg} of 32.3 Å^2). However, the piperazine and the trifluormethylphenyl, although visible, have averaged thermal factors of 45.1 and 55.7 Å^2, respectively, indicating a zone with higher flexibility, probably because of the absence of H-bonds to the protein residues.

The electron density maps are generally of good quality, except for a few polar side chain residues on the surface. Ninety-one percent of the residues lie in most favored regions and 8.5% in additional allowed regions. Only one residue, Tyr68, falls in a disallowed region. This amino acid is found in a tight loop connecting strand β1 and helix αA, which is involved in the cosubstrate binding site formation. Interestingly, this residue also shows ϕ and ψ values outside the expected range for other methyltransferases (MT) for which the three-dimensional structure is known. In some cases, a smaller residue, such as Ala or Gly, occupies this position.

COMT is a one-domain α/β protein. It consists of a mixed seven-stranded β-sheet flanked by five α-helices on one side and three helices on the other side. The strands are arranged in the order 3-2-1-4-5-7-6, where strand 7 is antiparallel to the other. A ribbon representation of the overall fold is presented in Fig. 10. The submission of the apo-protein coordinates to the DALI server (Holm and Sander, 1993) matched COMT with several SAM-dependent methyltransferases, namely DNA-, RNA-, protein- and small molecule-MT. Despite the very low amino acid sequence identity among MT, between 6 and 14%, they show structural homology [for a recent review on the structural and evolutionary aspects of SAM-MT, see Fauman et al. (1999)]. The other aligned structures are mostly proteins involved in oxidoreduction processes, such as dehydrogenases and reductases, some of which are NAD(P)- or FAD- dependent.

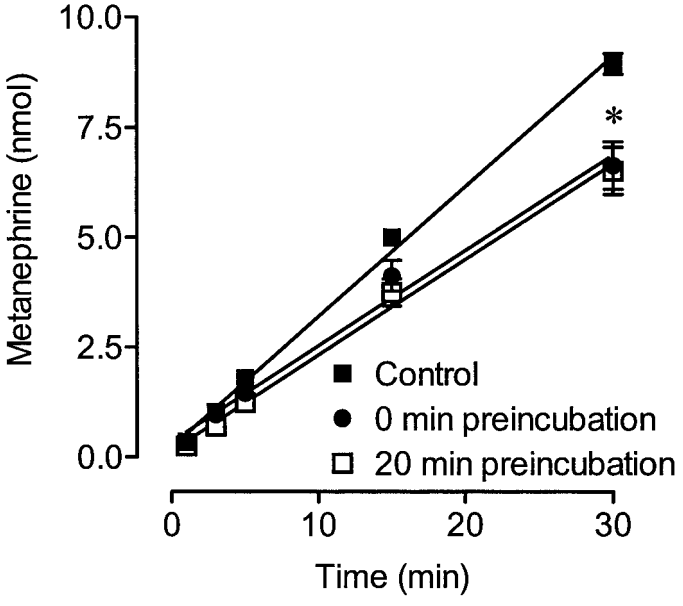

Fig. 7. Progress curves for the inhibition of S-COMT by BIA 3-335. S-COMT was incubated in the absence and in the presence of 300 nM of BIA 3-335 without preincubation or after a 20-min preincubation at 37°C. Reactions without preincubation were initiated with the enzyme and the others were started with the substrate. Each point represents the average of three independent determinations with S.E.M. Significantly different from the corresponding control values (*$P < 0.05$)

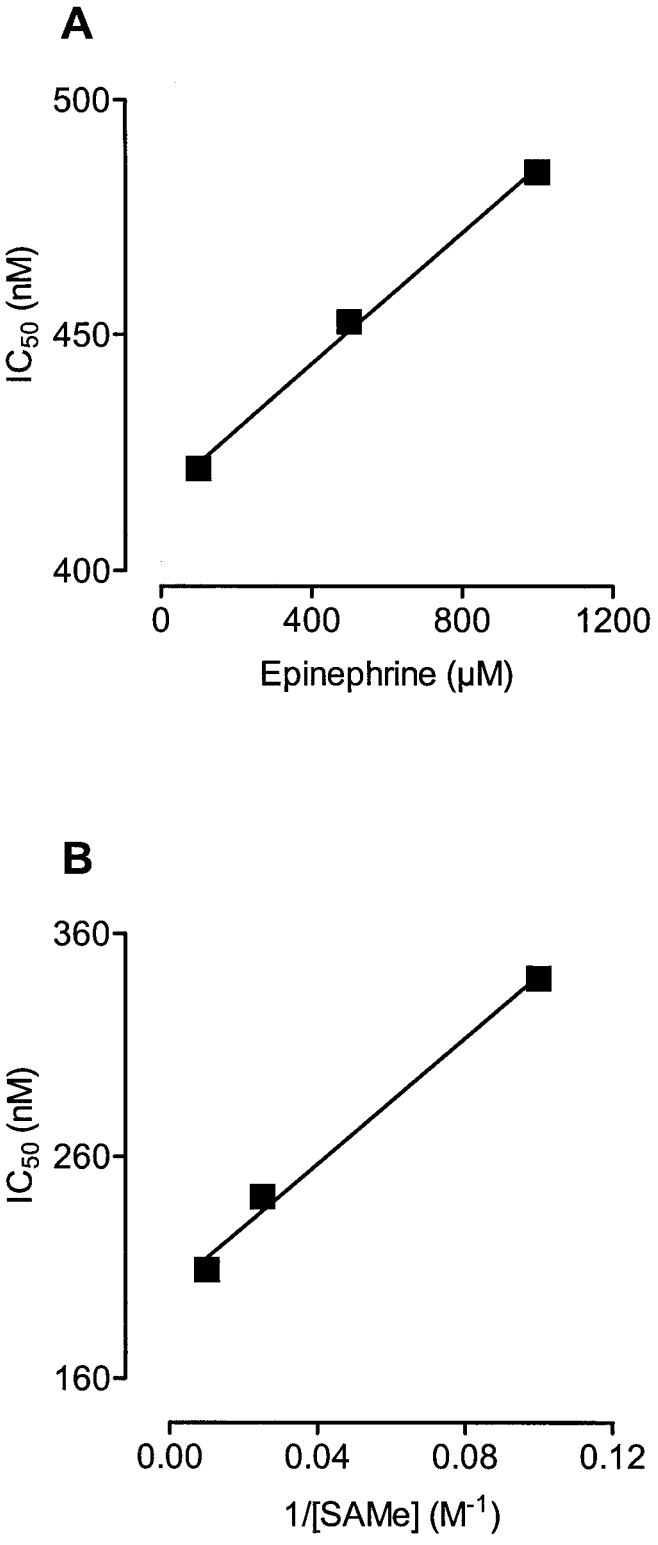

Fig. 8. Inhibition mechanism of S-COMT by BIA 3-335. A, plot of the IC_{50} values as a function of epinephrine concentration showing a competitive inhibition with catechol as substrate. B, plot of the IC_{50} values as a function of the reciprocal of SAM concentration, showing an uncompetitive pattern of inhibition. Reactions were initiated with the enzyme (520 nM). Results are the mean of three to five independent experiments.

Binding Mode of BIA 3-335 (Catalytic Site). The crystal structure of COMT in complex with BIA 3-335 shows that the inhibitor binds to the enzyme in a groove at the surface of the enzyme and that large substituents of the inhibitor extend out of the active site cavity toward the solvent, as represented in Fig. 11. Interestingly, the comparison of the molecular structure of BIA 3-335 determined independently with that of BIA 3-335 complexed with COMT reveals that the inhibitor undergoes a significant conformational change upon binding to the enzyme (Fig. 12). Although the active site has enough space to accommodate the X-ray structure of the unbound BIA 3-335, as depicted in Fig. 12, the inhibitor structural rearrangement is probably related to the optimization of interactions with the protein residues.

The nitrocatechol group of BIA 3-335 is the one responsible for "anchoring" the inhibitor to the enzymatic complex. Its coordination is similar to the one observed in the crystal structure obtained by Vidgren et al. (1994) and the two catechol hydroxyl groups are at hydrogen-bonding distances from the carboxylate of Glu199 and the zeta-nitrogen of Lys144. In contrast to the nitrocatechol moiety, the propanone carbon chain and the piperazine and trifluoromethylphenyl groups of BIA 3-335 are not hydrogen-bonded to the protein; rather, they interact mainly through hydrophobic contacts and have a higher thermal motion. A schematic representation of COMT interactions with the cofactor, inhibitor and Mg^{2+} ion is illustrated in Fig. 13.

There are some important protein residues that can establish hydrophobic contacts with the extended side chain of the inhibitor, such as Trp38, Pro174, and Met201. Met201 is the residue at the active site that has a different conformation in

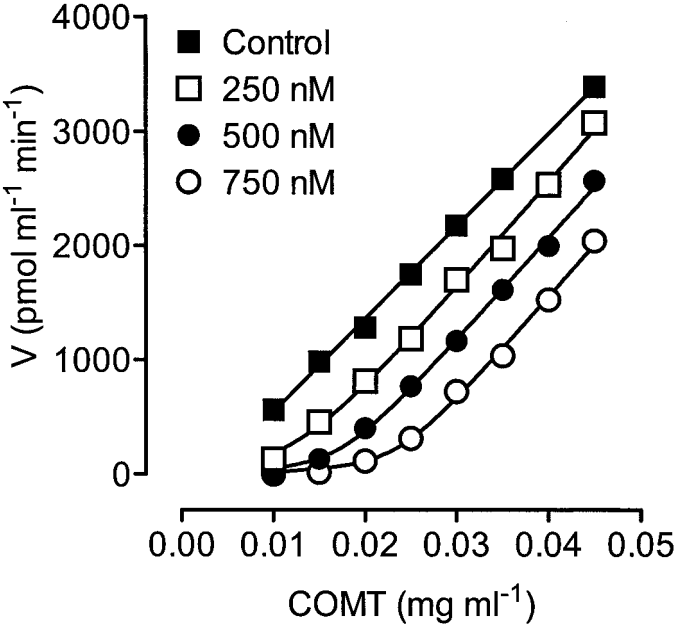

Fig. 9. Ackermann-Potter plot of S-COMT with BIA 3-335. Several concentrations of enzyme were incubated in the absence and in the presence of increasing concentrations of BIA 3-335 (250, 500, and 750 nM). The enzyme was preincubated with the inhibitor for 20 min and the reaction was started by the addition of 1000 μM epinephrine. Results are the mean of two independent experiments each performed in duplicate.

TABLE 1
Kinetic parameters for BIA 3-335
Values are means ± S.E.M. (n = 4) and were obtained by nonlinear regression analysis of eq. 1.

K_{cat} (per minute)	6.0 ± 1.1
ϵ	25,950 ± 3,907
K_i (nM)	6.0 ± 1.6
K_i^* (nM)	16.5 ± 4.3

K_{cat}, catalytic number, ϵ, molar equivalency; K_i, dissociation constant for enzyme-inhibitor complex; K_i^*, apparent K_i.

TABLE 2
Summary of data collection and refinement statistics
Values in parentheses refer to the outer resolution shell: 2.09 −2.02 Å.

Data collection	
Space group	$P3_221$
Unit cell parameters (Å,°)	a = b = 51.49, c = 168.29 a = β = 90, γ = 120
Solvent content (%)	~ 53
Resolution range (Å)	21.4 – 2.0
Total no. of reflections	131542
No. of unique reflections	17663
Redundancy	7.4
Completeness (%)	98.9 (95.3)
I/σ(I)	9.2 (2.2)
R-merge (%)	11.3 (48.3)
Refined model	
R-factor (%)	17.4
R-free (%)	19.8
Number of non-H atoms in:	
Protein molecule	1685
Water	85
SAM	27
BIA 3-335	31
Mg^{2+}	1
Average B-factor (Å^2)	
Main-chain atoms	22.1
Side-chain atoms	24.8
Water molecules	33.3
SAM	17.2
BIA 3–335	39.7
Mg^{2+} ion	17.6

TABLE 3
Crystal and structure refinement data

Empirical formula	$[C_{20}H_{21}F_3N_3O_5]^+[Br_{0.315}Cl_{0.685}]^-$
Formula weight	489.85
Temperature (° K)	293(2) K
Wavelength (Å)	1.54180 (Ni-filtered Cu Kα radiation)
Diffractometer	Nonius CAD-4
Crystal system	monoclinic
Space group	$P2_1/c$
Unit cell dimensions (Å, °)	a = 7.3969(4) b = 26.2002(15) c = 11.2216(9) β = 102.493(5)
Volume (Å^3)	2123.3(2)
Z	4
Density (calculated, Mg/m^3)	1.532
Absorption coefficient (per millimeter)	2.512
F(000)	1007
θ-range for data collection (°)	3.37 to 61.98
Index ranges	$-2 \le h \le 8$ $0 \le k \le 30$ $-12 \le l \le 12$
Reflections collected	3732
Independent reflections	3340 [R(int) = 0.0242]
Reflections observed [I>2σ(I)]	2560
Refinement method	Full-matrix least-squares on F^2 with SHELXL-97
Data / restraints / parameters	3340 / 30 / 320
Goodness-of-fit on F^2	1.081
Final R indices [I>2σ(I)]	R_1 = 0.0423 wR_2 = 0.1149
R indices (all data)	R_1 = 0.0608 wR_2 = 0.1201

COMT/BIA3-335 and COMT/dinitrocatechol (Vidgren et al., 1994). Of particular relevance is Trp38, which is located edge-to-face with the catechol plane, allowing for an important aromatic hydrophobic contact. In fact, the position of Trp38 may also favor interactions with the extended side chain of the inhibitor, which could contribute to the stabilization of the enzymatic complex. The important role of Trp38 for the high-affinity binding of catechol compounds is further supported by experiments comparing the enzymatic behavior of COMT isolated from rat and human versus pig, which has an arginine residue instead of tryptophan at position 38 (Piedrafita et al., 1990; Perez et al., 1994), where the pig enzyme binds the substrate and nitrocatechol inhibitors with a much lower affinity (10- to 100-fold lower) than the rat and human enzyme.

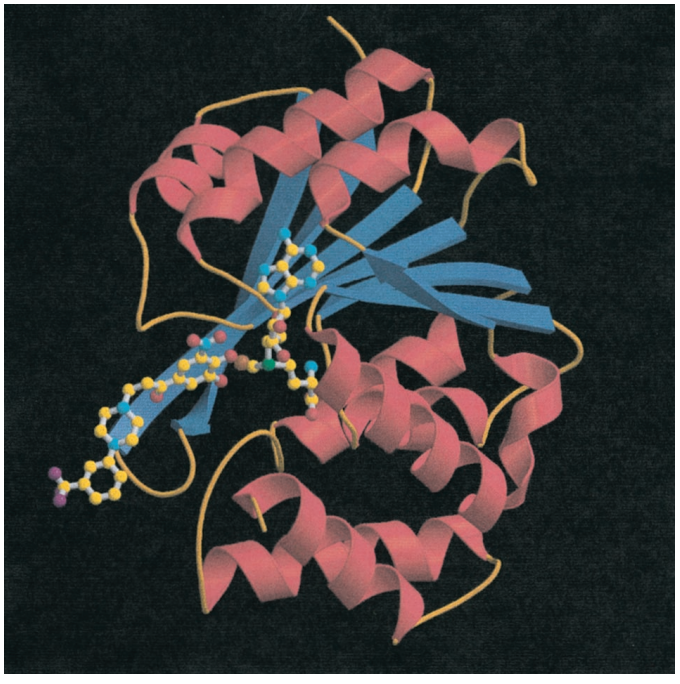

Fig. 10. Ribbon diagram of the three-dimensional structure of the COMT complexed with the cofactor SAM, the inhibitor BIA 3-335 and the Mg^{2+} ion. α-Helices are red, β-strands are blue, and the Mg^{2+} ion is brown. SAM and the inhibitor BIA 3-335 are shown as ball-and-stick models. Figure drawn using the programs Molscript (Kraulis, 1991) and Raster3D (Merrit and Murphy, 1994).

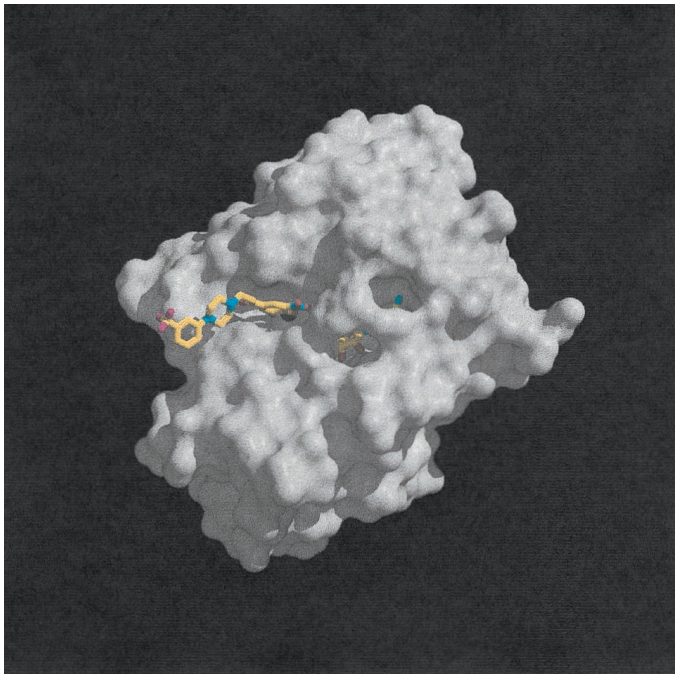

Fig. 11. Molecular surface of COMT shown in gray and white, with SAM and BIA 3-335 represented in stick. The Mg^{2+} ion is depicted in dark green. Figure drawn using programs GRASP (Nicholls et al., 1993) and Raster3D (Merrit and Murphy, 1994).

The Mg^{2+} is octahedrally coordinated to the side-chain oxygen atoms of residues Asp141, Asp169, Asn170, the two oxygen atoms of the catechol, and a water molecule. This ion plays the important structural role of orienting the hydroxyl groups of catechol and the activated methyl group of SAM into a reactive conformation (Fig. 13).

SAM Binding Site. The binding site of the methyl donor cofactor is situated within a deeper pocket of the enzyme, as illustrated in Fig. 11. The COMT residues involved in interactions with SAM are depicted in Fig. 13 and are conserved compared with the COMT-SAM-dinitrocatechol complex (Vidgren et al., 1994). Loop β1-αA contains the consensus sequence (GAxxG in COMT) associated with SAM binding in MT (Schluckebier et al., 1995). The acidic residue at position 90 (Glu90 in COMT) is a highly conserved residue within the SAM-dependent MT family. This is the last residue of strand β2, and its carboxylate oxygens are H-bonded to SAM ribose hydroxyls. Adenine has favorable van der Waals interactions with Met91, His142, and Trp143, whereas the ribose ring lies near Trp143 (Fig. 13). The activated sulfur of SAM is only 3.6 Å apart from the sulfur atom of Met40. As a result of the various H-bonds and van der Waals contacts, SAM is in the correct orientation for the methylation to take place and also shows a high affinity to COMT with a dissociation constant of 23 μM (Schluckebier et al., 1995).

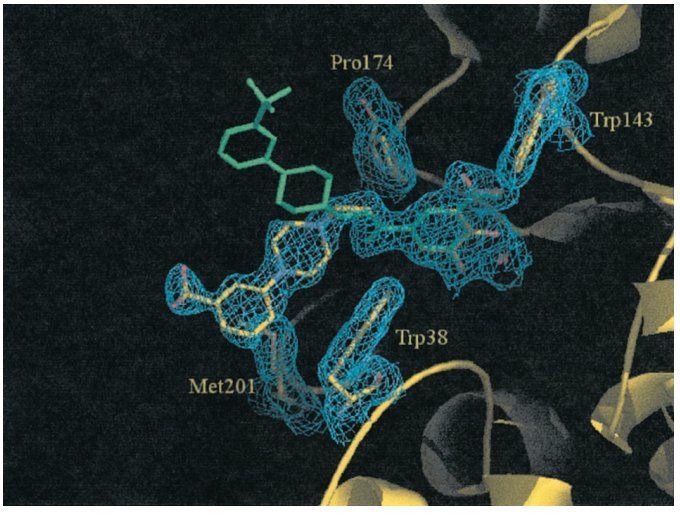

Fig. 12. Superposition of the X-ray structures of BIA 3-335 (represented in green) versus its conformation when complexed with COMT (colored by atom type: yellow, carbon; red, oxygen; blue, nitrogen; orange, sulfur; pink, fluorine). The electron density map, contoured at 1.2 σ, is represented for the inhibitor cocrystallized with the enzyme and four neighboring residues (Trp38, Trp143, Pro174 and Met201). Figure drawn with PyMOL Molecular Graphics System (DeLano Scientific, San Carlos, CA).

Discussion

The interest in COMT as a therapeutic target for Parkinson's disease and the limited beneficial effects observed in parkinsonian patients with tolcapone (liver toxicity) and entacapone (low efficacy) has led to the search and development of other inhibitor molecules that could be clinically useful (Perez et al., 1992; Brevitt and Tan, 1997; Masjost et al., 2000). BIA 3-335 was recently developed as a potent and selective COMT inhibitor (Learmonth and Soares-da-Silva, 2002). BIA 3-335 is endowed with a long duration of action and acts mainly as a peripheral COMT inhibitor with limited access to brain. The first property would allow a more appropriate regimen in the therapy patients afflicted with Parkinson's disease, namely by decreasing in a sustained manner the *O*-methylation of L-DOPA and improving its delivery to the brain, as has been observed with other COMT inhibitors (Parada et al., 2001). The second property limits the potentiation of brain dopaminergic stimulation, which can be evidenced by the appearance of abnormalities in motor activity and/or psychiatric symptoms (Parada and Soares-da-Silva, 2000a,b).

In the present work, the interactions of BIA 3-335 with recombinant rat S-COMT were characterized by evaluating the inhibition kinetics and by solving the three-dimensional structure of the complex enzyme-inhibitor-SAM. The results obtained with the recombinant form of rat liver S-COMT showed a Michaelis-Menten behavior for both the catechol (epinephrine) and the methyl donor (SAM) substrates, with kinetic parameters similar to those described in the literature for the native enzyme (Schultz and Nissinen, 1989; Borges et al., 1997; Vieira-Coelho and Soares-da-Silva, 1999). It is also shown that BIA 3-335 is a potent and reversible COMT inhibitor. This is evidenced by the findings that BIA 3-335 produces marked COMT inhibition at concentrations comparable with that of the enzyme and loses the inhibitory effect after gel filtration through PD-10 columns. The observation that inhibition of COMT by BIA 3-335 occurred at concentrations comparable with that of the enzyme points out to a tight-binding behavior. This is also confirmed by the asymptotic concave-up shapes of the Ackermann-Potter plots (Cha, 1975; Williams and Morrison, 1979). A reversible tight-binding inhibitor is one that exerts its effect on an enzyme-catalyzed reaction at a concentration comparable with that of the enzyme. Therefore, the plot of velocity against enzyme concentration at different inhibitor concentrations (Ackermann-Potter plot) is a useful method for detecting tight-binding inhibition. The plot of the steady-state velocity against the total enzyme concentration at different BIA 3-202 concentrations are asymptotic, concave-up curves and the velocity curve parallels to the control curve at sufficiently high enzyme concentrations, demonstrating the tight-binding nature of the inhibition (Cha, 1975). From Ackerman-Potter representations, it is also possible to determine the catalytic number (K_{cat}) and the molar equivalency (HE) of the enzyme. The K_{cat} is a measure of the efficiency of the enzyme because it gives the number of molecules of substrate converted into product by active site per unit of time. K_{cat} values for the recombinant form of rat liver S-COMT (6.0 ± 1.1/min) determined from the Ackerman-Potter plot, obtained with BIA 3-335, are in agreement with those described for the native form of rat liver S-COMT (4.5 ± 0.4/min) obtained with tolcapone (Vieira-Coelho and Soares-da-Silva, 1999), another tight-binding COMT inhibitor (Borges et al., 1997). The inhibitory effect of BIA 3-335 was not changed by preincubation times. The product formation (metanephrine) increased as a linear function of time and no differences were observed in metanephrine formation rates with 0 or 20 min preincubation. In addition, linearity of progress curves was observed in the presence of BIA 3-335 (300 nM), when the reaction was initiated with the enzyme, which indicates that the steady-state velocities were reached within the first minute of reaction (1 min was the first time point evaluated). This suggests that under the conditions tested equilibrium between the enzyme and the inhibitor was rapidly estab-

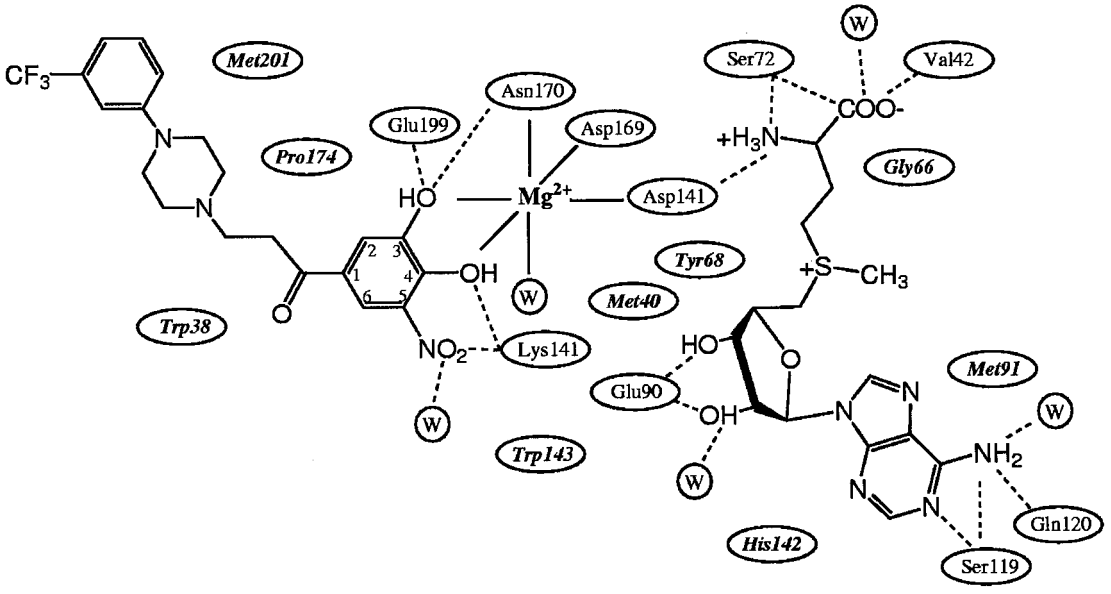

Fig. 13. Schematic representation of interactions at the active site between the cosubstrate SAM, Mg^{2+} ion, inhibitor BIA 3-335 and protein residues. Hydrogen bonds are indicated by dotted lines, and the Mg^{2+} coordination by solid lines. The residues making hydrophobic contacts are depicted in italic. The water molecules are represented as W.

lished. BIA 3-335 displayed a competitive type of inhibition to the substrate binding site and an uncompetitive type of inhibition to the SAM binding site with a K_i value of 6.0 ± 1.6 nM. It has also been shown that other nitrocatechol derivatives endowed with marked inhibitory activity against COMT, such as tolcapone, [2-(3,4-dihydroxy-2-nitrophenyl-)vinyl]phenylketone, and entacapone display the same type of inhibition mechanism (Schultz and Nissinen, 1989; Perez et al., 1994; Borges et al., 1997; Vieira-Coelho and Soares-da-Silva, 1999). This is probably related to the fact that the SAM binding site is deep in the COMT structure, whereas the substrate binding site is located on the surface of the enzyme and is easily accessible.

The overall structure of COMT complexed with SAM and BIA 3-335 (Fig. 10) is identical to that observed for this enzyme in complex with SAM and inhibitor 3,5-dinitrocatechol (Vidgren et al., 1994) The root-mean-square deviation is 0.16 Å for main chain atoms and 0.45 Å for all protein atoms. The residues of the protein involved in the interactions with the cosubstrate SAM, the nitrocatechol group of the inhibitor, and Mg^{2+} ion are the same as in the structure reported previously. BIA 3-335 binds into the catalytic site, which is in agreement with the results obtained in the functional studies. Based on the crystal structure, it seems that substituents have sufficient space to accommodate within the protein structure, either with side-chain substitution at C1 position, as in the case of BIA 3-335 and also tolcapone and entacapone or at C6, as in 2-[(3,4-dihydroxy-2-nitrophenyl-)vinyl]phenylketone (Vidgren and Ovaska, 1997). The C2 position of the catechol ring is hindered by steric constraints by the proline side chain, which is only ~4 Å apart. Two hydroxyl groups and one nitro group occupy the other carbon positions. The presence of Mg^{2+} is required for the catalysis to occur. On one hand, it has a structural role, organizing the active site and bringing together the SAM and the catechol substrate. On the other hand, the Mg^{2+} ion has also a functional role, to facilitate the deprotonation of the catechol hydroxyl and lower the p*K*a of Lys144, where its side-chain NH_2 is proposed to act as the catalytic base to abstract the proton from the hydroxyl group of catechol (Zheng and Bruice, 1997). Lysine is suggested to play a similar role in other enzymes, such as serine peptidase (Paetzel and Dalbey, 1997; Paetzel et al., 1997) and aspartate aminotransferase (Toney and Kirsch, 1989). The deprotonated hydroxyl ion would then react with the activated methyl group of SAM, forming methylcatechol and *S*-adenosylhomocysteine. However, inhibitors with a nitrocatechol structure, such as BIA 3-335, are generally very poor substrates, even though they bind well to the active site. This is because of the electronegative nitro group that strongly stabilizes the ionized catechol-COMT complex, thus increasing the activation energy of the methylation step (Vidgren and Ovaska, 1997; Ovaska and Yliniemelä, 1998). The structure of COMT with another inhibitor, OR-1840, has been mentioned in the literature (Vidgren et al., 1999), but because its coordinates are not deposited at the Protein Data Bank, their structural comparison is not possible. More recently, rat soluble COMT complexed with a bisubstrate nitrocatechol inhibitor was described (Lerner et al., 2001), the analysis of which suggests that both the protein and the inhibitor show a structural arrangement similar to that described here. The structure now presented is the first showing the interactions of a larger molecule within the active site. Whereas the noncatechol moiety of the bisubstrate inhibitor extends toward the SAM binding site, the BIA 3-335 side chain extends into the opposite direction. In fact, the BIA 3-335 side chain lays within a long groove, where interaction with hydrophobic residues are prevalent. The analysis of the present structure is expected to provide useful guidelines for the design of better inhibitors. For instance, the presence of hydrogen-bonding sites at the surface of the protein may help stabilizing long inhibitor side chains and compensate for the loss of entropy upon binding.

References

Bonifácio MJ, Vieira-Coelho MA, Borges N, and Soares-da-Silva P (2000) Kinetics of rat brain and liver solubilized membrane-bound catechol-O- methyltransferase. *Arch Biochem Biophys* **384:**361–367.

Bonifácio MJ, Vieira-Coelho MA, and Soares-da-Silva P (2001) Expression and characterization of rat soluble catechol-*O*-methyltransferase fusion protein. *Protein Expr Purif* **23:**106–112.

Bonifati V and Meco G (1999) New, selective catechol-O-methyltransferase inhibitors as therapeutic agents in Parkinson's disease. *Pharmacol Ther* **81:**1–36.

Borges N, Vieira-Coelho MA, Parada A, and Soares-da-Silva P (1997) Studies on the tight-binding nature of tolcapone inhibition of soluble and membrane-bound rat brain catechol-*O*-methyltransferase. *J Pharmacol Exp Ther* **282:**812–817.

Brevitt SE and Tan EW (1997) Synthesis and in vitro evaluation of two progressive series of bifunctional polyhydroxybenzamide catechol-O-methyltransferase inhibitors. *J Med Chem* **40:**2035–2039.

Brunger AT, Adams PD, Clore GM, DeLano WL, Gros P, Grosse-Kunstleve RW, Jiang JS, Kuszewski J, Nilges M, Pannu NS, et al. (1998) Crystallography & NMR system: A new software suite for macromolecular structure determination. *Acta Crystallogr Sect D Biol Crystallogr* **54:**905–921.

Cha S (1975) Tight binding inhibitors-I. Kinetic behavior. *Biochem Pharmacol* **24:** 2177–2185.

Ding YS, Gatley SJ, Fowler JS, Chen R, Volkow ND, Logan J, Shea CE, Sugano Y, and Koomen J (1996) Mapping catechol-O-methyltransferase in vivo: initial studies with [^{18}F]Ro41–0960. *Life Sci* **58:**195–208.

Fauman E, Blumenthal RM, and Cheng X (1999) Structure and evolution of AdoMet-dependent methyltransferases, in *S-Adenosylmethionine-Dependent Methyltransferases: Structures and Functions* (Cheng X and Blumenthal RM eds) pp 1–38, World Scientific, River Edge, NJ.

Gasparini M, Fabrizio E, Bonifati V, and Meco G (1997) Cognitive improvement during Tolcapone treatment in Parkinson's disease. *J Neural Transm* **104:**887–894.

Holm L and Sander C (1993) Protein structure comparison by alignment of distance matrices. *J Mol Biol* **233:**123–138.

Karhunen T, Tilgmann C, Ulmanen I, Julkunen I, and Panula P (1994) Distribution of catechol-*O*-methyltransferase enzyme in rat tissues. *J Histochem Cytochem* **42:**1079–1090.

Kraulis (1991) MOLSCRIPT: a program to produce both detailed and schematic plots of protein structures. *J Appl Crystallogr* **23:**946–950.

Lautala P, Ulmanen I, and Taskinen J (2001) Molecular mechanisms controlling the rate and specificity of catechol *O*-methylation by human soluble catechol *O*-methyltransferase. *Mol Pharmacol* **59:**393–402.

Learmonth DA and Soares-da-Silva P (2002) inventors, Portela & Ca., S.A., assignee. Novel substituted nitrocatechols, their use in the treatment of some central and peripheral nervous system disorders and pharmaceutical compositions containing them. Patent Cooperation Treaty patent WO 01/98251 A1. 2001 Dec 27.

Lerner C, Ruf A, Gramlich V, Masjost B, Zürcher G, Jakob-Roetne R, Borroni E, and Diederich F (2001) X-ray crystal structure of a bisubstrate inhibitor bound to enzyme catechol-O-methyltransferase: a dramatic effetc of inhibitor preorganization on a binding affinity. *Angew Chem Int Ed* **40:**4040–4042.

Lotta T, Vidgren J, Tilgmann C, Ulmanen I, Melén K, Julkunen I, and Taskinen J (1995) Kinetics of human soluble and membrane-bound catechol O- methyltransferase: a revised mechanism and description of the thermolabile variant of the enzyme. *Biochemistry* **34:**4202–4210.

Lundström K, Salminen M, Jalanko A, Savolainen R, and Ulmanen I (1991) Cloning and characterization of human placental catechol-O- methyltransferase cDNA. *DNA Cell Biol* **10:**181–189.

Lundström K, Tenhunen J, Tilgmann C, Karhunen T, Panula P, and Ulmanen I (1995) Cloning, expression and structure of catechol-O-methyltransferase. *Biochim Biophys Acta* **1251:**1–10.

Männistö PT and Kaakkola S (1999) Catechol-O-methyltransferase (COMT): biochemistry, molecular biology, pharmacology and clinical efficacy of the new selective COMT inhibitors. *Pharmacol Rev* **51:**593–628.

Männistö PT and Kaakkola S (1989) New selective COMT inhibitors: useful adjuncts for Parkinson's disease? *Trends Pharmacol Sci* **10:**54–56.

Männistö PT and Kaakkola S (1990) Rationale for selective COMT inhibitors as adjuncts in the drug treatment of Parkinson's disease. *Pharmacol Toxicol* **66:**317–323.

Männistö PT, Kaakkola S, Nissinen E, Linden IB, and Pohto P (1988) Properties of novel effective and highly selective inhibitors of catechol-O-methyltransferase. *Life Sci* **43:**1465–1471.

Männistö PT, Lang A, Rauhala P, and Vasar E (1995) Beneficial effects of co-administration of catechol-O-methyltransferase inhibitors and L-dihydroxyphenylalanine in rat models of depression. *Eur J Pharmacol* **274:**229–233.

Männistö PT, Ulmanen I, Lundström K, Taskinen J, Tenhunen J, Tilgmann C, and Kaakkola S (1992) Characteristics of catechol O-methyl-transferase (COMT) and properties of selective COMT inhibitors. *Prog Drug Res* **39:**291–350.
Masjost B, Ballmer P, Borroni E, Zürcher G, Winkler FK, Jakob-Roetne R, and Diederich F (2000) Structure-based design, synthesis and in vitro evaluation of bisubstrate inhibitors for catechol O-methyltransferase (COMT). *Chemistry* **6:**971–982.
Merrit E and Murphy MEP (1994) Raster3D Version 2.0. A program for photorealistic molecular graphics. *Acta Crystallogr Sect D Biol Crystallogr* **50:**869–873.
Moreau J-L, Borgulya J, Jenck F, and Martin JR (1994) Tolcapone: a potential new antidepressant detected in a novel animal model of depression. *Behav Pharmacol* **5:**344–350.
Morrison JF (1969) Kinetics of the reversible inhibition of enzyme-catalysed reactions by tight-binding inhibitors. *Biochem Biophys Acta* **185:**269–286.
Nicholls A, Bharadwaj R, and Honig B (1993) GRASP: graphical representation and analysis of surface properties. *Biophys J* **64:**A166.
Ovaska M and Yliniemelä A (1998) A semiempirical study on inhibition of catechol O-methyltransferase by substituted catechols. *J Comput Aided Mol Des* **12:**301–307.
Paetzel M and Dalbey RE (1997) Catalytic hydroxyl/amine dyads within serine proteases. *Trends Biochem Sci* **22:**28–31.
Paetzel M, Strynadka NC, Tschantz WR, Casareno R, Bullinger PR, and Dalbey RE (1997) Use of site-directed chemical modification to study an essential lysine in Escherichia coli leader peptidase. *J Biol Chem* **272:**9994–10003.
Parada A, Loureiro AI, Vieira-Coelho MA, Hainzl D, and Soares-da-Silva P (2001) BIA 3–202, a novel catechol-O-methyltransferase inhibitor, enhances the availability of L-DOPA to the brain and reduces its O-methylation. *Eur J Pharmacol* **420:**27–32.
Parada A and Soares-da-Silva P (2000a) BIA 3–202 does not potentiate amphetamine-induced dopaminergic hyperactivity (Abstract). *Br J Pharmacol* **131**:50P.
Parada A and Soares-da-Silva P (2000b) BIA 3–202 does not potentiate locomotor hyperactivity during increased dopaminergic stimulation (Abstract). *Br J Pharmacol* **131**:49P.
Perez RA, Fernandez-Alvarez E, Nieto O, and Piedrafita FJ (1992) Dihydroxynitrobenzaldehydes and hydroxymethoxynitrobenzaldehydes: synthesis and biological activity as catechol-O-methyltransferase inhibitors. *J Med Chem* **35:**4584–4588.
Perez RA, Fernandez-Alvarez E, Nieto O, and Piedrafita FJ (1994) Kinetics of the reversible tight-binding inhibition of pig liver catechol-O-methyltransferase by [2-(3,4-dihydroxy-2- nitrophenyl)vinyl]phenyl ketone. *J Enzyme Inhib* **8:**123–131.
Piedrafita FJ, Elorriaga C, Fernandez-Alvarez E, and Nieto O (1990) Inhibition of catechol-O-methyltransferase by *N*-(3,4-dihydroxyphenyl)maleimide. *J Enzyme Inhib* **4:**43–50.
Rajput AH, Martin W, Saint-Hilaire MH, Dorflinger E, and Pedder S (1997) Tolcapone improves motor function in parkinsonian patients with the "wearing-off" phenomenon: a double-blind, placebo-controlled, multicenter trial. *Neurology* **49:** 1066–1071.
Rinne UK, Larsen JP, Siden A, and Worm-Petersen J (1998) Entacapone enhances the response to levodopa in parkinsonian patients with motor fluctuations. *Neurology* **51:**1309–1314.
Rivett AJ, Francis A, and Roth JA (1983) Localization of membrane-bound catechol-O-methyltransferase. *J Neurochem* **40:**1494–1496.
Rodrigues ML, Archer M, Bonifacio MJ, Soares-da-Silva P, and Carrondo MA (2001) Crystallization and preliminary crystallographic characterization of catechol-O-methyltransferase in complex with its cosubstrate and an inhibitor. *Acta Crystallogr Sect D Biol Crystallogr* **57:**906–908.
Roussel A and Cambilau C (1989) *Silicon Graphics Geometry Partner Directory*, Silicon Graphics, Mountain View, CA.
Salminen M, Lundström K, Tilgmann C, Savolainen R, Kalkkinen N, and Ulmanen I (1990) Molecular cloning and characterization of rat liver catechol-O- methyltransferase. *Gene* **93:**241–247.
Schluckebier G, O'Gara M, Saenger W, and Cheng X (1995) Universal catalytic domain structure of AdoMet-dependent methyltransferases. *J Mol Biol* **247:**16–20.
Schultz E and Nissinen E (1989) Inhibition of rat liver and duodenum soluble catechol-O- methyltransferase by a tight-binding inhibitor OR-462. *Biochem Pharmacol* **38:**3953–3956.
Sheldrick GM (1997) Patterson superposition and ab initio phasing. *Methods Enzymol* **276:**628–641.
Tenhunen J, Salminen M, Jalanko A, Ukkonen S, and Ulmanen I (1993) Structure of the rat catechol-O-methyltransferase gene: separate promoters are used to produce mRNAs for soluble and membrane-bound forms of the enzyme. *DNA Cell Biol* **12:**253–263.
Tenhunen J, Salminen M, Lundstrom K, Kiviluoto T, Savolainen R, and Ulmanen I (1994) Genomic organization of the human catechol O-methyltransferase gene and its expression from two distinct promoters. *Eur J Biochem* **223:**1049–1059.
Tenhunen J and Ulmanen I (1993) Production of rat soluble and membrane-bound catechol O- methyltransferase forms from bifunctional mRNAs. *Biochem J* **296:** 595–600.
Toney MD and Kirsch JF (1989) Direct Bronsted analysis of the restoration of activity to a mutant enzyme by exogenous amines. *Science (Wash DC)* **243:**1485–1488.
Vidgren J and Ovaska M (1997) Structural aspects in the inhibitor design of catechol *O*-methyltransferase, in *Structure-Based Drug Design* (Veerapandian P ed) pp 343–363, Marcel Dekker, Inc., New York.
Vidgren J, Ovaska M, Tenhunen J, Tilgmann C, Lotta T, and Männistö PT (1999) Catechol *O*-methyltransferase, in *S-Adenosylmethionine-Dependent Methyltransferases: Structures and Functions* (Cheng X and Blumenthal RM eds) pp 55–91, World Scientific Publishing, River Edge, NJ.
Vidgren J, Svensson LA, and Liljas A (1994) Crystal structure of catechol O-methyltransferase. *Nature (Lond)* **368:**354–358.
Vieira-Coelho MA and Soares-da-Silva P (1999) Effects of tolcapone upon soluble and membrane-bound brain and liver catechol-O-methyltransferase. *Brain Res* **821:** 69–78.
Waters CH, Kurth M, Bailey P, Shulman LM, LeWitt P, Dorflinger E, Deptula D, and Pedder S (1997) Tolcapone in stable Parkinson's disease: efficacy and safety of long-term treatment. *Neurology* **49:**665–671.
Williams JW and Morrison JF (1979) The kinetics of reversible tight-binding inhibition. *Methods Enzymol* **63:**437–467.
Zheng YJ and Bruice TC (1997) A theoretical examination of the factors controlling the catalytic efficiency of a transmethylation enzyme - catechol O-methyltransferase. *J Am Chem Soc* **119:**8137–8145.
Zürcher G, Keller HH, Kettler R, Borgulya J, Bonetti EP, Eigenmann R, and Da Prada M (1990) Ro 40–7592, a novel, very potent and orally active inhibitor of catechol-O-methyltransferase: a pharmacological study in rats. *Adv Neurol* **53:** 497–503.

Address correspondence to: Dr. Patrício Soares-da-Silva, Department of Research and Development, BIAL, Av. da Siderurgia Nacional, 4745–457 S. Mamede do Coronado, Portugal. E-mail: psoares.silva@bial.com